10298 *Biochemistry* **2010,** *49,* 10298–10307
DOI: 10.1021/bi101018c

BIOCHEMISTRY
including biophysical chemistry & molecular biology
Article

Targeting of Protein Phosphatases PP2A and PP2B to the C-Terminus of the L-Type Calcium Channel $Ca_v1.2$[†]

Hui Xu,[‡,§,∥] Kenneth S. Ginsburg,[§] Duane D. Hall,[‡] Maike Zimmermann,[‡,§] Ivar S. Stein,[‡,§] Mingxu Zhang,[‡,§] Samvit Tandan,[⊥] Joseph A. Hill,[⊥] Mary C. Horne,[‡,§] Donald Bers,[§] and Johannes W. Hell*[,‡,§]

[‡]*Department of Pharmacology, University of Iowa, Iowa City, Iowa 52242-1109, United States,* [§]*Department of Pharmacology, University of California, Davis, California 95616-8636, United States,* [∥]*Department of Pharmacology, Norman Bethune College of Medical Sciences, Jilin University, Changchun, Jilin 130021, China, and* [⊥]*Department of Internal Medicine (Cardiology), University of Texas Southwestern Medical Center, Dallas, Texas 75390-8573, United States*

Received June 24, 2010; Revised Manuscript Received November 3, 2010

ABSTRACT: The L-type Ca^{2+} channel $Ca_v1.2$ forms macromolecular signaling complexes that comprise the β_2 adrenergic receptor, trimeric G_s protein, adenylyl cyclase, and cAMP-dependent protein kinase (PKA) for efficient signaling in heart and brain. The protein phosphatases PP2A and PP2B are part of this complex. PP2A counteracts increase in $Ca_v1.2$ channel activity by PKA and other protein kinases, whereas PP2B can either augment or decrease $Ca_v1.2$ currents in cardiomyocytes depending on the precise experimental conditions. We found that PP2A binds to two regions in the C-terminus of the central, pore-forming α_1 subunit of $Ca_v1.2$: one region spans residues 1795−1818 and the other residues 1965−1971. PP2B binds immediately downstream of residue 1971. Injection of a peptide that contained residues 1965−1971 and displaced PP2A but not PP2B from endogenous $Ca_v1.2$ increased basal and isoproterenol-stimulated L-type Ca^{2+} currents in acutely isolated cardiomyocytes. Together with our biochemical data, these physiological results indicate that anchoring of PP2A at this site of $Ca_v1.2$ in the heart negatively regulates cardiac L-type currents, likely by counterbalancing basal and stimulated phosphorylation that is mediated by PKA and possibly other kinases.

Ca^{2+} influx through L-type channels controls membrane excitability (*1*), synaptic plasticity (*2*−*5*), and gene expression (*6*, *7*) in neurons and triggers myocardial contraction in the heart. L-type Ca^{2+} channels are the main targets of so-called organic calcium channel blockers, which include dihydropyridines, phenylalkylamines, and benzothiazepines. Voltage-gated Ca^{2+} channels consist of a central ion-conducting pore, the α_1 subunit, and auxiliary α_2−δ, and β subunits (*8*). $Ca_v1.2$ containing the central $\alpha_1 1.2$ is the main L-type channel in the cardiovascular system, heart, and brain (*8*).

$Ca_v1.2$ is a point of convergence of multiple regulatory pathways. For instance, β-adrenergic stimulation upregulates our heart beat in part via phosphorylation of $Ca_v1.2$ by PKA[1] (*9*, *10*). $Ca_v1.2$ phosphorylation and dephosphorylation are highly dynamic with phosphatases reversing the stimulatory effect of PKA and perhaps other kinases rather quickly (*11*, *12*). We found earlier that PP2A and PP2B (calcineurin) are constitutively bound to $Ca_v1.2$ (*13*, *14*). Channel-associated PP2A reverses PKA-mediated phosphorylation of serine 1928 (*13*). Serine 1928 is one of two identified PKA sites in $\alpha_1 1.2$, the other being the most recently identified serine 1700 (*15*, *16*). Although phosphorylation of serine 1928 is not necessary for regulation of $Ca_v1.2$ possibly because other phosphorylations can suffice in its absence (*8*, *15*−*18*), it is highly regulated and continues to serve as indicator for PKA-mediated phosphorylation of $\alpha_1 1.2$.

We now narrow down the exact binding sites for PP2A to two short regions (residues 1795−1818 and 1965−1971) that independently bind PP2A. PP2B binds immediately downstream of residues 1965−1971 without competition between these two phosphatases for binding to this rather narrow region. A peptide that disrupts binding of PP2A but not PP2B to this site increases L-type-mediated Ca^{2+} currents in cardiomyocytes, likely by preventing the inhibitory effect of PP2A under basal and ISO[1]-stimulated conditions.

EXPERIMENTAL PROCEDURES

Materials, Antibodies, and Peptides. ECL and ECL-Plus detection kits and glutathione Sepharose were purchased from Amersham Pharmacia Biotech (Piscataway, NJ). The monoclonal mouse anti-GST antibody was from NeuroMAB (Davis, CA), the monoclonal mouse anti-PP2A/C antibody 1D6 (*19*) from Upstate Biotechnology (Lake Placid, NY), the monoclonal rat antibody 6F9 from Dr. G. Walter (*20*), and the monoclonal mouse anti-PP2B antibody (*21*, *22*) from BD Transduction Laboratories. The anti-$\alpha_1 1.2$ antibody had been produced against a segment of the cytosolic loop between domains II and III of $\alpha_1 1.2$, as described (*23*). Peptides for displacement studies were custom synthesized by CHI Scientific (Maynard,

[†]This work was supported by Grant [2007] 3020 from the China Scholarship Council (to H.X.), National Institutes of Health Research Grants R01-NS035563 and R01-AG017502 (to J.W.H.), R01-GM056900 (to M.C.H.), R01-HL075173 (to J.A.H.), and R37-HL30077 (to D.B.), and American Heart Association Grants 0535235N (to D.D.H.) and (0640084N) (to J.A.H.).

*To whom correspondence should be addressed at the Department of Pharmacology, University of California. Tel: (530) 752 6540. Fax: (530) 752 7710. E-mail: jwhell@ucdavis.edu.

[1]Abbreviations: GST, glutathione *S*-transferase; ISO, isoproterenol; PAGE, polyacrylamide gel electrophoresis; PKA, cAMP-dependent protein kinase; PP, protein phosphatase; PVDF, polyvinyl difluoride; SDS, sodium dodecyl sulfate.

 Published on Web 11/05/2010

MA). Other chemicals were of standard biochemical quality and from usual commercial suppliers.

Peptide Array Overlay Assay. The peptide spot array spanning residues 1784−2067 of rabbit cardiac $\alpha_1$1.2 (for sequence see GenBank accession number CAA33546) was synthesized on a PVDF membrane as published (*24*). The first spot contains a 15-mer peptide covering residues 1784−1798 of $\alpha_1$1.2. Peptides in each subsequent spot were shifted by one residue from the previous spot. The PVDF membrane was blocked with 10% milk powder in TBS (10 mM Tris-HCl, pH 7.4, 150 mM NaCl) before incubation with recombinant PP2A/C subunit expressed in *Escherichia coli* (see below) in the same solution, washed, and probed with the anti-PP2A/C antibody.

In Vitro Binding Assays of 6×His-PP2A and PP2B to GST Fusion Proteins. GST-CT-8 encoding residues 1909−2029 of rabbit heart $\alpha_1$1.2 (*13*) served as a template for construction of GST fusion proteins covering residues 1909−1946 (CT-8-1), 1909−1971 (CT-8-2), 1943−2029 (CT-8-3), and 1969−2029 (CT-8-4) and for a point mutation on the otherwise full-length GST-CT-8 construct to change Ala1959 to Pro (GST-CT-8-P), as described (*14*). GST-CT-B containing residues 1694−1817 of rat $\alpha_1$1.2 cDNA (*25*) (nearly identical to residues 1726−1849 of the above rabbit $\alpha_1$1.2) was as given earlier (*13*). These GST fusion proteins as well as the 6×His-PP2A/C construct (*26*) were expressed in Nova Blue (Novagen, Madison, WI) and BL21 Star (Invitrogen, San Diego, CA) *E. coli* strains and purified and used for *in vitro* pull-down interaction studies as detailed previously (*13*, *14*, *26*). PP2B was expressed in *E. coli* and purified for pull-down experiments as outlined earlier (*14*, *27*). For quantification of pull-down experiments, film exposures of immunoblots were digitalized with an Epson Perfection 4180 Photo flatbed scanner and scanned immunosignals quantified by densitometry in Adobe Photoshop. Multiple exposures with increasing time length were taken to ensure that signals were in the linear range (for more details see refs *13* and *28*). In Figures 3−6 and Supporting Information Figure 1, immunosignals were normalized relative to the signals from the corresponding positive control samples obtained with GST-CT-8, CT-8-3, or CT-B in the absence of peptide. Means and SEMs were calculated and analyzed with Prism 3.0 (GraphPad Software, Inc.). Differences were accepted as significant at $p < 0.05$ by paired *t* test.

Immunoprecipitation. Mouse (C57black/6) hearts and brains were homogenized in 2.5 mL of ice-cold solubilization buffer (10 mM Tris-HCl, pH 7.4, 150 mM NaCl, 1% Triton X-100, 10 mM EDTA, 10 mM EGTA, plus protease inhibitors 1 μg/mL pepstatin A, 10 μg/mL leupeptin, 20 μg/mL aprotinin, 8 μg/mL each calpain inhibitors I and II) before centrifugation at ~250000*g* for 30 min. Aliquots (200 μL) of the supernatants were incubated with 2 μg of the anti-$\alpha_1$1.2 antibody or of nonspecific control IgG and 10 μL of prewashed protein A Sepharose slurry (50% resin, 50% buffer) for 4−6 h and washed three times with 1% Triton X-100 in TBS (10 mM Tris-HCl, pH 7.4, 150 mM NaCl) containing 0.1% SDS and once with 10 mM Tris-HCl, pH 7.4. Proteins were extracted by SDS sample buffer, separated by SDS−PAGE, transferred to PVDF membrane, and detected as above.

PP2A and PP2B Activity Assays. PP2A catalytic activity was assessed using the DuoSet IC (R&D Systems) malachite green/molybdate-based PP2A activity assay (*29*, *30*) in accordance with the manufacturer's instructions. Murine cardiac tissue was homogenized in lysis buffer 8 (50 mM HEPES, 0.1 mM EGTA, 0.1 mM EDTA, 120 mM NaCl, 0.5% NP-40, pH 7.5, 25 μg/mL leupeptin, 25 μg/mL pepstatin, 2 μg/mL aprotinin, 1 mM PMSF) and nonsoluble material removed by centrifugation at ~170000*g* for 30 min. PP2A was immobilized on microtiter plate wells from lysate (500 μg of total protein per well) using an anti-PP2A/C antibody (Millipore 05-421), washed, and preincubated with 20 μM peptide 1, 4, or 5 at room temperature for 15 min before addition of 200 μM final concentration synthetic phosphopeptide substrate (DLDVPIPGRFDRRVS(PO3)VAAE). After 30 min at 37 °C, malachite green and molybdate were added to bind free phosphate and initiate the colorimetric reaction (*29*, *30*). Light absorbance was measured at 630 nm. The amount of released phosphate was calculated from standard curves generated in parallel using orthophosphate. To exclude that another phosphatase present in the lysate bound to the wells and contributed to the activity or that phosphate contaminations contributed to the final read out, lysate was either omitted or PP2A was blocked in some assays with 10 nM okadaic acid (IC_{50} of 0.2−2.5 nM for PP2A (*31*)), which is specific for PP2A at this concentration (*32*).

PP2B/calcineurin activity was determined using the malachite green/molybdate-based calcineurin assay kit from Calbiochem following the manufacturer's instructions. Purified calmodulin (CaM, 250 nM final concentration) was incubated with 40 units of recombinant PP2B and 20 μM peptide 1, 4, or 5 at room temperature for 15 min. A synthetic phosphopeptide substrate (DVPIPGNFDNNVS(PO_3)VAAE) was then added (150 μM final concentration). After 40 min at 37 °C, malachite green and molybdate were added to determine how much phosphate had been released as described for PP2A. For negative control to exclude contamination by external phosphate either PP2B or calmodulin was omitted.

Electrophysiology. For recording I_{Ca}(L), freshly prepared adult rabbit ventricular myocytes were preincubated in Na^+- and Ca^{2+}-free Tyrode solution (140 mM LiCl, 1 mM $MgCl_2$, 10 mM HEPES-free acid, 1 mM EGTA, 10 mM glucose; pH = 7.4 with LiOH) for 15−20 min and then plated on laminin-treated glass coverslips in Ca^{2+}-free solution containing 4 mM CsCl, 1 mM $MgCl_2$, 10 mM HEPES-free acid, 140 mM tetraethylammonium (TEA)-Cl, and 10 mM glucose (pH = 7.4 with TEA-OH). For experiments, 2 mM $CaCl_2$ was added to the TEA bath solution. Predepletion of cytosolic Na^+ and use of Na^+-free solutions allowed recording of I_{Ca}(L) free of interference by Na/Ca exchange or voltage-gated Na channels. In most experiments, cells were preincubated with thapsigargin (1 μM, 15 min) to block Ca^{2+} loading of the sarcoplasmic reticulum and niflumic acid (30 μM) to block Cl^- currents.

Ca^{2+} current was recorded at room temperature (22−24 °C) in the whole cell perforated patch configuration using β-escin (*33*). Pipets were tip-filled with solution containing 100 mM *N*-methyl-glucamine (NMG), 20 mM TEA-Cl, 80 mM glutamic acid (free acid), 10 mM HEPES-free acid, 5.66 mM $MgCl_2$, 5 mM ATP (Tris salt), 0.3 mM GTP (Li^+ salt), 5 mM EGTA, and 1.09 mM $CaCl_2$, resulting in a calculated free [Ca^{2+}] = 50 nM (Max-Chelator). pH was adjusted with HCl to 7.2. Use of EGTA buffering was intended to prevent global but not local [Ca^{2+}] changes. This same solution with β-escin (predissolved in H_2O; final concentration 50 μM in pipet) and either peptide 1, 4, or 5 (for nomenclature, see Results and Figure 1B; final [peptide] 50 μM) or no peptide added was used to backfill pipets. The liquid junction potential of the pipet solution, 9 mV, pipet negative, was corrected.

After cells were sealed it took usually 15−20 min for the formation of β-escin pores, which are of sufficient size to provide

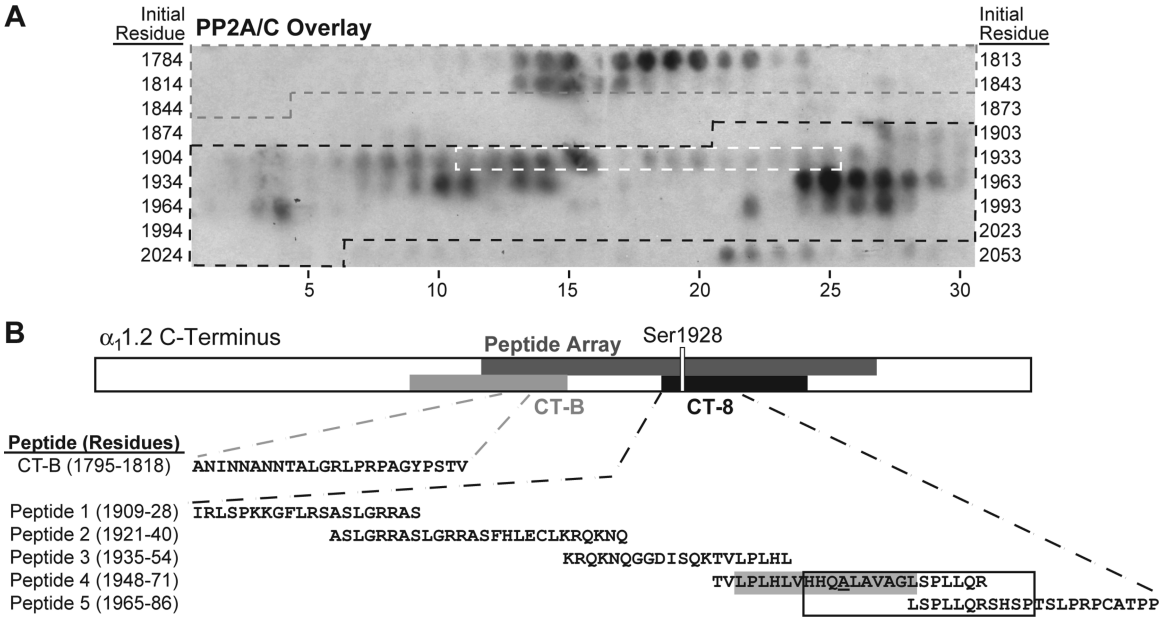

FIGURE 1: PP2A/C strongly binds to $\alpha_1$1.2 residues 1795−1818 and 1956−1975 in peptide array overlay. (A) A peptide array spanning residues 1784−2067 of rabbit heart $\alpha_1$1.2 was incubated with the catalytic C subunit of PP2A (PP2A/C) and probed with anti-PP2A/C antibodies. Peptides encompassing residues from CT-B (gray), CT-8 (black), and Ser1928 (white) are indicated by dashed outlines on the overlay image. (B) Topology of the linearized $\alpha_1$1.2 C-terminus depicting the region covered by the peptide array (dark gray) and GST fusion proteins CT-B (gray) and CT-8 (black), the latter including Ser1928. Below are tabulated the sequence of the residues that define the PP2A binding region in CT-B according to the overlay and the CT-8 derived peptides 1−5 used for the displacement studies below. The boxed residues in peptides 4 and 5 are those that are encompassed by the PP2A/C binding-positive peptides on the array in the CT-8 region. The putative α-helix is shaded gray with Ala1959 underlined in peptide 4.

electrical access as well as access of molecules of ~10 kDa including our peptides (*34*). We confirmed that fluorescent dextran (M_r ~10 kDa) and hence our peptides could pass through the β-escin pores (not illustrated). Cells were continuously held under voltage clamp, with series resistance (typically 8−10 megΩ) compensated by ~75%. Depolarizations (200 ms) to 0 mV from −90 mV were applied each 10 s, under control condition ([ISO] = 0) and then at 10, 55, and 300 nM ISO. ISO (300 nM) was prepared fresh for each session from the same sample and diluted successively. Each [ISO] was maintained ≥3 min, to apparent steady state. At each [ISO] a current−voltage relationship was also recorded, using 200 ms depolarizations from −90 mV to between −40 and +50 mV. Cells were held at −90 mV for 1−2 s between steps to ensure full recovery of channels from inactivation. Control experiments showed that 1 mM $CdCl_2$ blocked the current identified as I_{Ca}(L) (not illustrated). Upon washout of ISO at the end of an experiment, I_{Ca}(L) returned on average to 83% of its initial value.

The transient parts of currents evoked by repeated depolarization to 0 were measured. Each individual trace was first corrected for leak conductance (initial holding current/initial holding voltage). Then we found the difference between peak current (identified directly) and final asymptotic current, obtained by fitting the postpeak decay phase of the current to

$$I = A(k \exp(-t/\tau_1) + (1-k)\exp(-t/\tau_2)) + C$$

where I is the observed current, A is the identified peak, and the fit parameters were k ($0 < k < 1$, a weighting factor), τ_1, and τ_2 (time constants), and C was a constant. As I_{Ca}(L) inactivates almost completely, constant C was usually near 0 (this procedure limits errors due to any uncorrected leakage or junctional potential-related fluxes). Current−voltage data were treated similarly, with all currents normalized to cell membrane capacitance.

Peak current−voltage data were fit to a Boltzmann function

$$I = [G_{max}/(1 + \exp((V_{50} - V_m)/K_V)](V - E_{rev}) + C$$

where I is the observed current and V_m is the test depolarization potential, while the fit parameters are G_{max} (maximum conductance), V_{50} (half-activation potential), K_V (voltage dependence slope factor), E_{rev} (net current reversal potential), and C (offset and residual leak correction constant).

We statistically analyzed the influence of ISO and the choice of peptide on G_{max} and V_{50} using two-way analysis of variance (ANOVA; GraphPad Prism software v5.02, www.graphpad.com).

RESULTS

Peptide Array Overlay with PP2A/C. Pull-down experiments with GST fusion proteins previously identified two different regions in the C-terminus of $\alpha_1$1.2 that mediate direct binding of the catalytic subunit of PP2A (PP2A/C) (*13*). One region lies within residues 1726−1849 and the other within residues 1909−2029 of the rabbit heart $\alpha_1$1.2 as defined by pull down with GST-CT-B and -CT-8 fusion proteins, respectively (*13*). To identify the binding sites more precisely, we used a solid-phase peptide library. Overlay with the catalytic subunit of PP2A (PP2A/C) expressed in *E. coli* as poly-His fusion protein revealed two regions with especially strong immunoreactivity. One region encompasses residues 1795−1818 of $\alpha_1$1.2 (ANINNANNTALGRLPRPAGYPSTV; residue numbering as for the original $\alpha_1$1.2 sequence from rabbit heart; GenBank accession number CAA33546). This segment is within the original CT-B segment (Figure 1). The other region comprises residues 1956−1975 (HHQALAVAGLSPLLQRSHSP) within the original CT-8 segment (Figure 1). Experiments described below suggest that all other regions on the peptide array that show detectable immunoreactivity are not strong constitutive PP2A/C interaction sites.

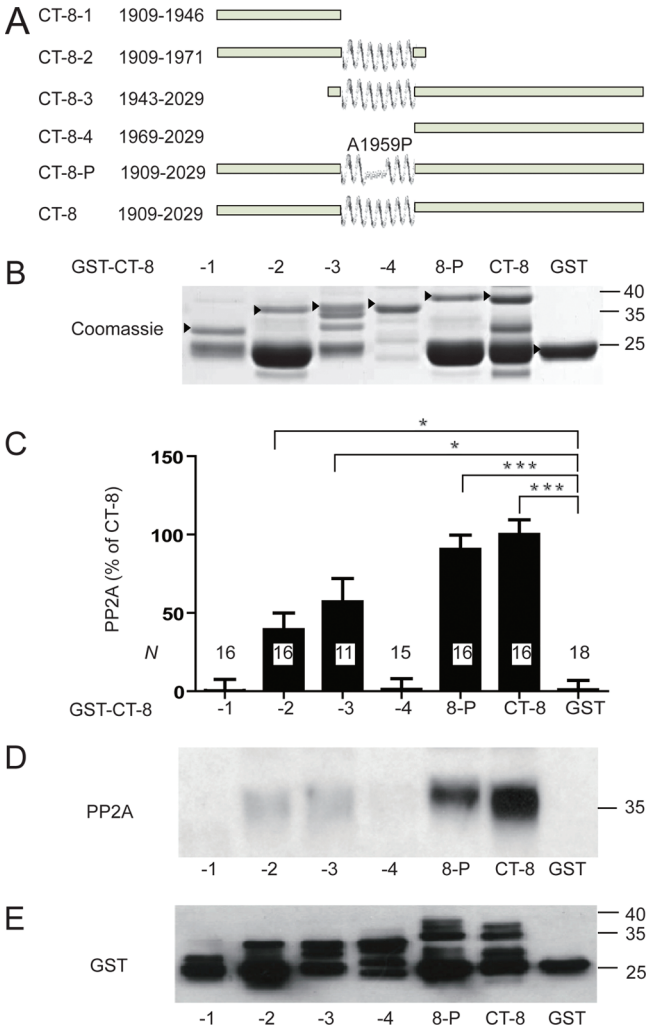

FIGURE 2: PP2A/C binds to the central region spanning residues 1943−1971 in CT-8. (A) Schematic of the parental CT-8 segment (bottom) and its derivatives. A predicted α-helix is indicated in the center of CT-8 and all derivatives that contain this segment. CT-8P encodes CT-8 with the Ala1959Pro mutation as depicted above the presumably interrupted α-helix. (B) SDS−PAGE of the various purified GST-CT-8 fusion proteins including GST itself as detected by Coomassie staining. Arrowheads indicate expected positions of the corresponding full-length polypeptides. (C−E) Pull down of purified poly-His-PP2A/C with the fusion proteins as detected by immunoblotting with anti-PP2A/C (D). Results from 18 different experiments were quantified. Means ± SEM from *N* samples for each condition are graphed in (C) (*, $p < 0.05$; ***, $p < 0.001$). Reprobing with anti-GST was routinely performed to confirm that similar amounts of GST fusion proteins were present (E).

PP2A/C Pull-Down Experiments with GST Fusion Proteins. We recently provided evidence that residues 1943−1971 within CT-8 bind yet another phosphatase, the Ca^{2+}- and calmodulin-activated PP2B (calcineurin) (*14*). To define the PP2A binding site within this region relative to PP2B, we used shorter fragments of GST-CT-8 (Figure 2A). The Robson−Garnier algorithm predicts that this region forms an α-helix (*14*). In fact, substituting Ala1959 with Pro, a helix breaker, abrogates PP2B binding (*14*). All fusion proteins were first purified on glutathione Sepharose, eluted, and dialyzed to remove glutathione for immobilization of comparable amounts of protein on glutathione Sepharose and subsequent PP2A/C pull-down experiments. Several fusion proteins were partially cleaved, resulting in a substantial amount of GST with only minimal or no additional channel segments (Figure 2B,E). To allow comparison between the different fusion proteins, equal amounts of the corresponding full-length forms (arrowheads in Figure 2B; see also Figure 2E) were loaded onto the resin. To determine the portion of PP2A/C binding to CT-8 fusion proteins that was specific, pure GST was loaded in parallel roughly matching the amount of the former. Background was typically less than 20% and was subtracted from total binding signals for CT-8 pull-down samples. PP2A/C bound consistently and with high specificity to full-length CT-8 as well as the proline mutant CT-8-P (Figure 2C,D). This equivalent interaction of CT-8 and CT-8-P with PP2A/C is in striking contrast to PP2B binding, which was abrogated by the proline mutation (*14*). PP2A/C did not specifically bind to CT-8-1 or CT-8-4, N-terminal and C-terminal truncations of the original CT-8 fusion protein that lacked the putative α-helix (Figure 2C,D). PP2A/C binding to CT-8-2 and CT-8-3 (both contained the putative α-helical region, residues 1943−1971) was more variable but showed significant specific binding ($p < 0.05$ compared to GST control) albeit weaker than to the full-length CT-8.

CT-8-1 encodes residues 1909−1946 and includes the first regions that showed weak binding in the peptide overlay assay (starting with residue 1910; Figure 1). Because CT-8-1 did not show any specific binding in the pull-down test, the modest binding to the 1910 region in the Figure 1 overlay assay likely indicates only weak association. Because this region contains Ser1928, which is phosphorylated by PKA and dephosphorylated by PP2A, this binding could indicate a catalytic site interaction (*13*), which would typically be brief in nature. Similarly, the weak signal in the PP2A/C overlay for peptides that cover residues 1988−2005 is also likely either nonspecific or limited in nature as CT-8-4 encoding residues 1969−2029 did not show any specific binding in the pull-down experiments.

Peptide Competition Experiments with PP2A/C and CT-8. We used synthetic peptides in solution to further define the PP2A/C binding site in CT-8. Peptides were 20−24 residues long and covered various overlapping regions between residues 1909 and 1986 (peptides 1−5; Figure 1B). In the first set of experiments with peptides 1−4, only peptide 4 significantly inhibited pull down of PP2A/C by GST-CT-8 (Figure 3A,B). Peptide 4 covers the predicted α-helix in this region and most of the residues encompassed by the second strong binding region of the peptide array overlay experiment. We subsequently tested peptide 4 with Pro substituting the Ala at position 1959 (peptide 4P) and peptide 5, which includes the last 7 residues of peptide 4 plus 15 residues toward the C-terminus. Peptide 4P and peptide 5 also disrupted PP2A/C binding to CT-8 but not as strongly as peptide 4 (Figure 3C,D). Similar results were obtained in two experiments using GST-CT-8-3 for PP2A pull down (Figure 3E).

Peptides 1 and 2 cover the region starting with residue 1910 that showed some weak binding in the peptide array overlay assay. The finding that these peptides did not diminish at all pull down of PP2A/C by GST-CT-8 is further evidence for the above conclusion that this site interacts weakly if at all with PP2A. Subsequent attempts to further narrow down the precise binding site for PP2A within the sequence covered by peptides 4 and 5 with 10-mer peptides failed (Supporting Information Figure 1A, B; peptides 6−10). The most likely explanation is that the affinity of the shorter peptides for PP2A is too low for effective competition with the CT-8 polypeptide because none of these peptides might have a sufficient number of contact sites for PP2A even though we increased peptide concentration from 10 to

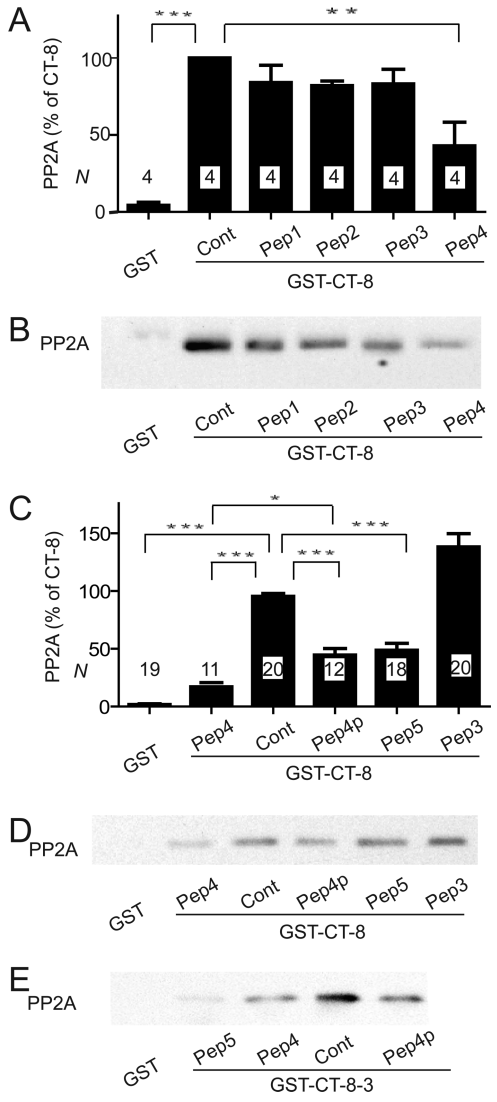

FIGURE 3: Peptides containing $\alpha_1$1.2 residues 1965−1971 (LSPLLQR) compete with GST-CT-8 for PP2A/C binding. Graphed are means ± SEM from *N* samples in four (A) and ten (C) independent experiments and representative immunoblots (B, D, E) of pull-down experiments of purified poly-His-PP2A/C with GST-CT-8 (A−D) or GST-CT-8-3 (E) with the indicated peptides (10 μM) present during PP2A binding (see Figure 1 for definition of peptides 1−5). GST served as negative control and GST-CT-8 or GST-CT-8-3 without any peptide as positive control (Cont; *, $p < 0.05$; **, $p < 0.01$; ***, $p < 0.001$).

20 μM (Supporting Information Figure 1) and in one experiment to 40 μM (data not shown).

Peptide Competition Experiments with PP2A/C and CT-B. To test whether the interactions of PP2A with CT-8 and CT-B are independent of each other, we performed peptide competition PP2A pull-down experiments with GST-CT-B. None of the CT-8-derived peptides reduced PP2A pull down by GST-CT-B, including peptides 4, 4P, and 5 (Figure 4). This result suggests that PP2A binds with different sites to CT-B and CT-8. Attempts to define the CT-B binding site with similar competition studies using two partially overlapping peptides derived from the peptide overlay experiment failed as one covering residues 1794−1808 was insoluble and the other one covering residues 1804−1818 had no effect (data not shown).

Peptide Competition Experiments with PP2B and CT-8. Because the Ala1959Pro mutation in the putative α-helix formed

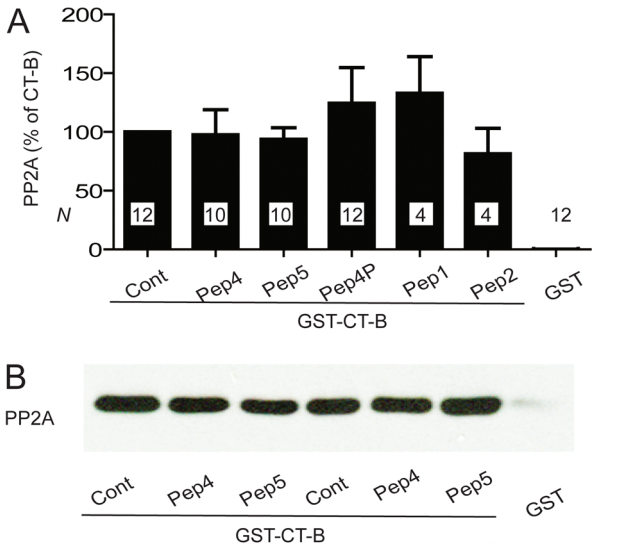

FIGURE 4: Peptides derived from CT-8 do not compete with GST-CT-B for PP2A/C binding. Graphed are means ± SEM from *N* samples in six independent experiments (A) and representative immunoblots (B) of pull-down experiments of purified poly-His-PP2A/C with GST-CT-B with the indicated peptides (10 μM) present during PP2A binding. GST was the negative control and GST-CT-B without any peptide the positive control (Cont).

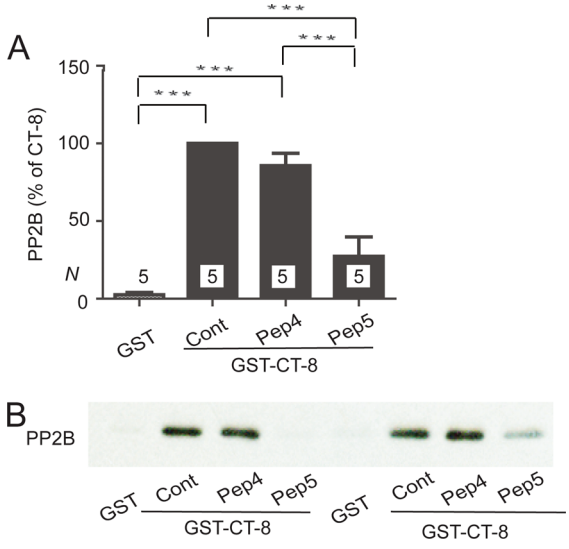

FIGURE 5: Peptide 5 but not peptide 4 competes with GST-CT-8 for PP2B binding. Graphed are means ± SEM from *N* samples in three independent experiments (A) and example immunoblot (shown in duplicate) of pull-down experiments of purified poly-His-PP2B with GST-CT-8 (B) with peptide 4 or 5 (10 μM) present as indicated during PP2B binding. GST was the negative control and GST-CT-8 without any peptide the positive control (Cont; ***, $p < 0.001$).

by residues 1943−1971 abrogated PP2B binding to GST-CT-8 (*14*), it appeared likely that PP2B binds at or near this region. In peptide competition studies analogous to those for PP2A above, only peptide 5 but not peptide 4 affected pull down of PP2B by GST-CT-8 (Figure 5). Peptide 4 covers nearly all of the putative α-helix including Ala1959, which is not part of peptide 5 (Figure 1B). It is possible that the Ala1959Pro mutation disrupts the conformation of the putative α-helix not only in its immediate vicinity but also downstream of it. Such a disruption could extend to residues covered by peptide 5. As the N-terminal seven residues of peptide 5 are also present on peptide 4, yet peptide 4 did not disrupt PP2B binding to CT-8, those residues appear not to be

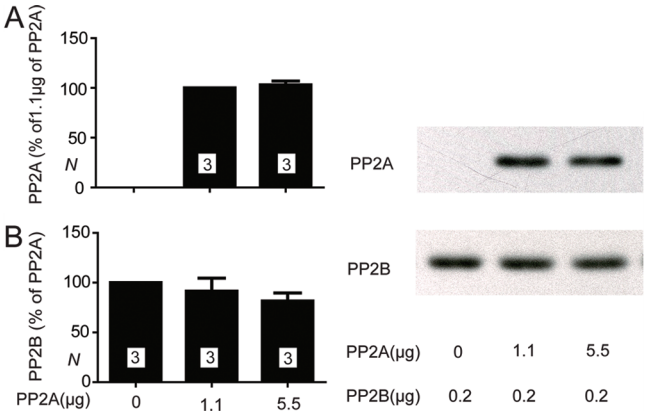

FIGURE 6: PP2A/C and PP2B do not compete for CT-8 binding. Glutathione Sepharose was sequentially incubated with GST-CT-8, then 0, 1.1, or 5.5 μg of PP2A, and finally 0.2 μg of PP2B. Representative immunoblots (left panels) illustrate the relative amount of PP2A (A) and PP2B (B) present in the same pull-down samples. Means ± SEM from three independent experiments are shown in the right panels.

sufficient for PP2B binding if they can participate at all in the interaction with PP2B. In any case, it appears that PP2B does not directly bind to the immediate vicinity of Ala1959 but rather somewhat downstream of it. We tested shorter peptides covering peptides 4 and 5, but similar to our PP2A results none affected PP2B binding (Supporting Information Figure 1C).

Competition Experiments between PP2A and PP2B. As the above peptide studies indicate that PP2A and PP2B bind to residues very close to each other in CT-8, we wondered whether these two phosphatases would compete for binding to this region. GST-CT-8 was immobilized on glutathione Sepharose and incubated with either 0, 1.1, or 5.5 μg of affinity-purified PP2A and subsequently with 0.2 μg of affinity-purified PP2B. Immunoblotting showed that the amount of PP2A bound to the GST-CT-8-charged resin was indistinguishable for the 1.1 vs 5.5 μg samples (Figure 6A). This observation indicates that both amounts allowed saturation of the immobilized CT-8 with PP2A. Subsequent incubation with PP2B resulted in comparable amounts of PP2B pulled down by the GST-CT-8 resin whether this resin was preincubated with PP2A or not (Figure 6B). These data suggest that PP2A and PP2B can simultaneously bind to CT-8.

Peptide 5 but Not Peptide 4 Displaces PP2A but Not PP2B from Native $Ca_v1.2$ Complexes. The above in vitro binding assays define the precise PP2A and PP2B binding sites on $\alpha_1$1.2. However, they do not show whether these peptides are effective in promoting dissociation of PP2A or PP2B from native $Ca_v1.2$ complexes. Dissociation of both phosphatases must be very slow as a substantial amount of them remains bound during the coimmunoprecipitation procedure, which takes at least 4 h after detergent extraction and dilution of tissue content. Peptides are thought to promote dissociation of otherwise relatively stable protein complexes by gaining access to interaction sites on the complementary binding partner upon partial unbinding. The latter would not lead to full dissociation itself unless interfering compounds prevent full rebinding. It is thus quite possible that some peptides compete during binding reactions but do not promote dissociation of preformed complexes.

Endogenous PP2A and PP2B coimmunoprecipitated with $Ca_v1.2$ (Figure 7). PP2A holoenzymes typically consist the catalytic C subunit, the scaffolding A subunit, and one of numerous B

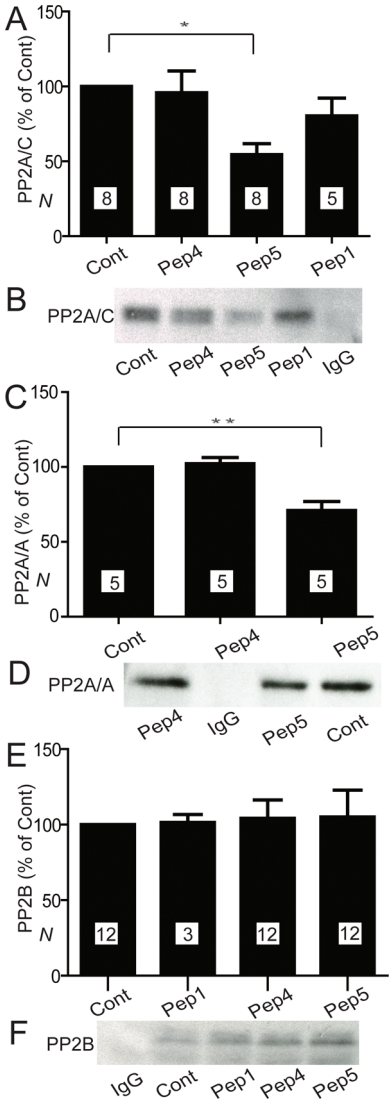

FIGURE 7: Peptide 5 displaces PP2A but not PP2B from native $Ca_v1.2$ complexes. Immunoprecipitations of $Ca_v1.2$ were performed in the absence (Cont) or presence of 20 μM peptide 1, 4, or 5 and PP2A/C (A, B), PP2A/A (C, D), or PP2B (E, F) detected by immunoblotting. Graphed are means ± SEM from *N* samples in eight (A), two (C), and six (D) independent experiments. Control precipitations with nonspecific IgG indicate the specificity of PPA/C (B), PP2A/A (D), and PP2B (F) coprecipitations with $Ca_v1.2$.

subunits, which mediate targeting of PP2A holoenzymes (*35*). We determined peptide effects on coimmunoprecipitations of PP2A/C as well as PP2A/A. All coprecipitations with $Ca_v1.2$ were specific for PP2A/C, PP2A/A, and PP2B as control IgG did not pull down any of these proteins (Figure 7B,D,F). Inclusion of peptide 5 but not of peptide 4 during the immunoprecipitation step reduced coprecipitation of PP2A/A and PP2A/C with $Ca_v1.2$ by ~50%. Neither peptide 5 nor peptide 4 affected coprecipitation of PP2B. These results indicate that only peptide 5 but not peptide 4 effectively dislocates PP2A from native $Ca_v1.2$ complexes even though both peptides compete during PP2A-GST-CT-8 association reactions. Despite its effect on PP2A, peptide 5 did not effectively dislodge PP2B from the endogenous $Ca_v1.2$ complex.

Perfusion of Cardiomyocytes with Peptide 5 but Not Peptide 4 Increases L-Type Ca^{2+} Currents. To determine the functional role of the PP2A anchoring site on $Ca_v1.2$, adult rabbit ventricular myocytes were freshly prepared and I_{Ca}(L) recorded

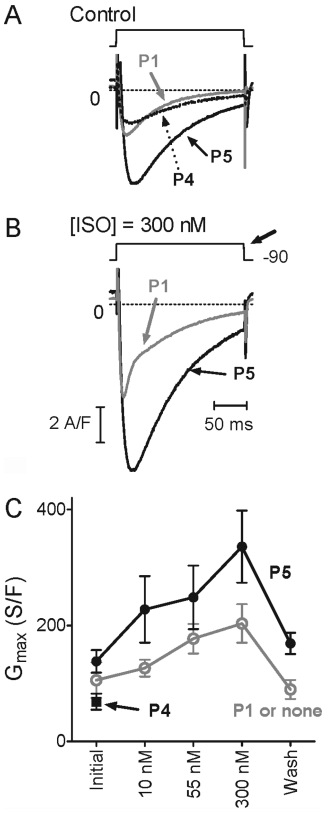

FIGURE 8: Peptide 5 increases I_{Ca}(L) density under control and ISO treatment conditions compared to peptide 1 or no peptide. (A) Representative current traces upon depolarization from −90 mV with peptide 1 (gray), peptide 4 (dotted), or peptide 5 (black) in the recording electrode ([ISO] = 0). (B) Traces from the same respective cells with [ISO] = 300 nM. Traces were obtained from the respective current−voltage relations, at the depolarization giving maximal peak current (bold arrow, B). The voltage for maximum current (typically −20 mV without ISO), which would be relevant for cardiac cell contraction, shifted negative in response to ISO (see Results). Traces were smoothed minimally, and vertically adjusted slightly, to plot asymptotic values at 0 (dashed lines). (C) Graphed are means ± SEM of maximum conductance G_{max} obtained by fit (see Experimental Procedures) from peak current−voltage relations. Each data point in (C) represents five to eight measurements, except wash ($N \geq 4$) from in total three cells with no peptide, four with peptide 1, nine with peptide 4, and seven with peptide 5. In several cells, data were not recorded at all [ISO]. We combined the three experiments with no peptide and the four with peptide 1 for our analyses as no differences between these two conditions were obvious (*, $p > 0.05$; Mann−Whitney (U) tests).

in a perforated patch configuration. The saponin-related mild detergent β-escin was used (*33*) because it affords access of peptides and polypeptides to the cell interior (*34*) (see Experimental Procedures). Inclusion of peptide 5, which displaces PP2A but not PP2B from endogenous $Ca_v1.2$ as determined by the above immunoprecipitation experiments, resulted in a larger I_{Ca}(L) compared to peptide 1 or no peptide (Figure 8A,C). We used peptide 1 as control because it has a charge content similar to that of peptides 4 and 5 but does not affect binding of PP2A or PP2B to CT-8 nor coimmunoprecipitation of PP2A or PP2B with native $Ca_v1.2$. ANOVA showed that the choice of peptide (none or 1 vs 4 vs 5) affected I_{Ca}(L) at all ISO concentrations, appearing in Figure 8C as the strong increase with peptide 5. Independently of the choice of peptide, ISO increased I_{Ca}(L), as expected. The effect of peptide 5 to increase basal $Ca_v1.2$ activity might reflect basal activity of a kinase, possibly PKA, that is unmasked by reducing local PP2A activity via disruption of phosphatase

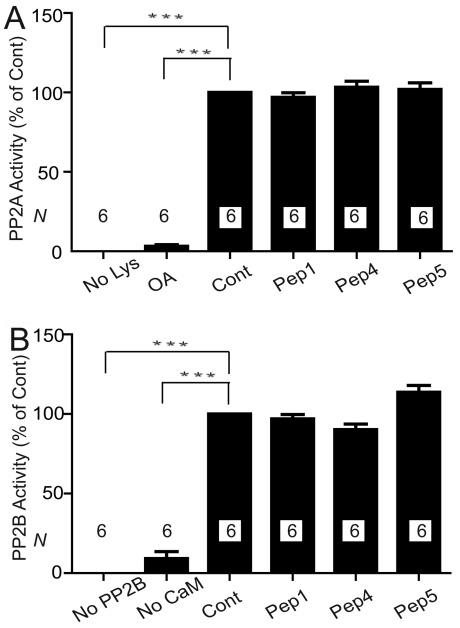

FIGURE 9: Peptides 1, 4, and 5 do not affect phosphatase activity of PP2A or PP2B. PP2A (immunoisolated from heart) and recombinant purified PP2B were preincubated with 20 μM peptide 1, 4, or 5, 10 nM okadaic acid (OA), which is a specific PP2A blocker at this concentration, or without any additives (positive control for full phosphatase activity; Cont). Respective phosphopeptide substrates were added for PP2A and PP2B assays, and subsequently phosphate release was determined. Lysate (No Lys; PP2A), PP2B (No PP2B), or calmodulin (No CaM) were omitted in some assays to test for phosphate contaminations from other ingredients. Shown are means ± SEM of phosphatase activity determined in two independent experiments with triplicate samples each ($N = 6$) for each phosphatase.

binding to the CT-8 region. The enhanced β-adrenergic stimulation with peptide 5 was seen over the full range of ISO concentrations as illustrated in example traces for [ISO] = 300 nM (Figure 8B) and as determined via G_{max} derived from I/V relations (Figure 8C). These findings indicate that endogenous PP2A is associated with $Ca_v1.2$ in cardiac myocytes to limit the magnitude of PKA-mediated enhancement of I_{Ca}(L). Half-activation potential V_{50} derived from the I/V relations shifted significantly negative on application of ISO as expected (*12*). This shift tended to be greater with peptide 5 (maximal shift −16.0 ± 1.9 mV SEM vs −12.9 ± 1.9 mV with peptide 1 or no peptide, but the difference was statistically not significant; not illustrated). In agreement with the lack of peptide 4 on PP2A coimmunoprecipitation with $Ca_v1.2$ from native tissue, peptide 4 did not affect I_{Ca}(L) (Figure 8A,C).

Peptides 4 and 5 Do Not Directly Affect PP2A or PP2B Catalytic Activity. To ensure that in the above recordings peptide 5 acted by displacing PP2A from $Ca_v1.2$ and not by inhibiting general phosphatase activity, we determined catalytic activity of purified PP2A and PP2B in the presence and absence of these peptides, with negative results (Figure 9).

DISCUSSION

Formation of inside-out patches from rabbit ventricular myocytes causes run down of L-type currents that is blocked by okadaic acid (*11*). This observation provided early functional evidence that a phosphatase is anchored in close proximity to the channel that counteracts upregulation of $Ca_v1.2$ by phosphorylation. We found that PP2A is associated with $Ca_v1.2$ (*36*) and

subsequently identified two attachment sites for PP2A within the C-terminus of the central $\alpha_1$1.2 subunit (*13*). In the present study pull-down experiments with CT-8-derived truncated fusion proteins indicate that the segment between residues 1943 and 1971 of $\alpha_1$1.2 is required for specific PP2A/C binding to this region. Our peptide overlay indicates that 15-mer peptides starting with residues 1956−1959 possess strong PP2A/C binding potential, with some peptides showing weaker binding. The core sequence common to all four strongly binding peptides is 1959ALAVAGLSPLLQ1970. Furthermore, peptide 4 and peptide 5 compete with CT-8 for PP2A/C binding. Both peptides contain the C-terminal six residues of that core sequence plus an additional Arg C-terminal to those residues (1965LSPLLQR1971). Finally, the Ala1959Pro mutation in CT-8 does not abrogate PP2A/C binding to CT-8 nor does this substitution in peptide 4 prevent the resulting peptide 4P from competing with CT-8 for PP2A/C pull down. The simplest explanation of all of these results is that the main interaction sites for PP2A/C in this region of $\alpha_1$1.2 are 1965LSPLLQ1970. This conclusion is in agreement with the finding that CT-8-3, which covers residues 1943−2029, but not CT-8-4, which covers residues 1969−2029, pulls down PP2A as the latter is lacking residues 1965−1968 from the core interaction site. Accordingly, residues 1965−1968 are critical for binding.

PP2A typically exists as a trimer consisting of a catalytic C subunit, a structural A subunit, and a B-type subunit (*35*). The >15 identified B-type subunits are subcategorized into three types (B, B′, and B″) (*35*, *37*, *38*). They generally mediate targeting of the PP2A holoenzyme to its substrates, which involves at least in some cases a stable interaction. It is thus remarkable that PP2A/C itself exhibits strong constitutive binding to two different sites on $\alpha_1$1.2 that possess different structural features. PP2A also forms a constitutive interaction with the type 2 ryanodine receptor in heart, which in this case is mediated via the B″ subunit PR130 (*39*). Ca_v1.2 and the ryanodine receptor are precisely juxtaposed in cardiomyocytes, allowing Ca^{2+} influx through Ca_v1.2 to rapidly and effectively induce Ca^{2+} release from the sarcoplasmic reticulum. The finding that both protein complexes individually anchor PP2A indicates that PP2A has to be precisely targeted to the individual proteins for effective dephosphorylation.

Whereas PP2A/C bound equally well to CT-8 and CT-8-P, PP2B only bound to CT-8 (*14*). Furthermore, peptides 4, 4P, and 5 all interfered with PP2A binding, but only peptide 5 inhibited PP2B binding to CT-8. The most parsimonious explanation for these results is that PP2B has its main attachment site immediately downstream of Arg1971. As discussed above, residues immediately upstream of Arg1971 (1965LSPLLQ1970) are most likely the main attachment site for PP2A. Because PP2A and PP2B can simultaneously bind to the region surrounding Arg1971, these upstream residues are obviously not critical for PP2B binding. Our earlier finding that CT-8-P has impaired PP2B binding is thus likely due to downstream secondary structural changes induced by the proline substitution, an alteration that could encompass residues C-terminal to Arg1971. We conclude that although PP2A and PP2B bind to the same region of $\alpha_1$1.2, binding is through interaction with different residues, which are in close proximity to each other.

Earlier evidence suggests that PP2A in general (*12*) and specifically when bound to the CT-8 region of $\alpha_1$1.2 downstream of Ser1928 (*13*) reduces Ca_v1.2 currents in the HEK-derived tsA-201 cells by counteracting PKA-mediated stimulation of these currents (*13*). Further, channel-associated PP2A reverses PKA-mediated phosphorylation of Ser1928 (*13*, *36*), which is still considered a valid readout of Ca_v1.2 phosphorylation by PKA even though it is not necessary for Ca_v1.2 regulation (*8*, *17*, *18*). In cardiomyocytes, three different modes of Ca_v1.2 activity have been defined (*40*). Channel openings are absent in mode 0, short in mode 1, and long in mode 2 with only relatively brief intermittent closures in this mode (*40*). β-Adrenergic signaling via PKA induces transition from mode 0 to mode 1 or 2 (*10*, *41*). Okadaic acid, which at submicromolar concentrations is more selective for PP2A than PP1, impairs the reversal of mode 2 and 1 in cardiac and smooth muscle cells, whereas application of PP2A to excised inside-out membrane patches promotes this reversal (*32*, *42*, *43*). Collectively, these findings indicate that PP2A reduces Ca_v1.2 activity at least in part by reversing PKA-mediated stimulation of Ca_v1.2. Our findings that peptide 5 displaces PP2A from native Ca_v1.2 and increases basal and ISO-enhanced I_{Ca}(L) now indicate that PP2A must be bound to the region containing residues 1965−1970 for effectively regulating Ca_v1.2 activity.

In contrast to PP2A inhibitors, several ventricular myocyte studies report that PP2B inhibition has either no detectable effect on I_{Ca}(L) in rat, mouse, or rabbit (*44*−*47*), decreases this current in rat (*14*, *48*), or, in one study, increases I_{Ca}(L) in mouse (*49*). The basis for these discrepant findings is unclear but raises the possibility that in ventricular myocytes PP2B does not regulate channel activity as robustly as PP2A with respect to the basal activity state of I_{Ca}(L) or PKA-dependent activation of I_{Ca}(L). Dissociation of PP2B from Ca_v1.2 should thus either have a limited effect on I_{Ca}(L) or even decrease it in ventriculocytes. The finding that perfusion of peptide 5 increased I_{Ca}(L) in our rabbit vetriculocytes and because peptide 5 dislodged only PP2A but not PP2B from Ca_v1.2 thus suggests that the peptide 5-induced increase in I_{Ca}(L) is largely due to displacement of PP2A from $\alpha_1$1.2 residues 1965−1971.

However, in neurons and HEK293 cells ectopically expressing Ca_v1.2, PP2B consistently acts to decrease L-type currents (*50*−*52*). Thus our previous findings (*14*), which are based on multiple lines of evidence leaving little doubt that PP2B stimulates I_{Ca}(L) in cardiomyocytes, could reflect that PP2B acts under certain conditions in cardiomyocytes not directly on Ca_v1.2 but rather on other regulators of this channels, perhaps PP2A itself. For instance, the B-type subunit B′δ (B56δ) is phosphorylated by PKA to increase the phosphatase activity of the corresponding PP2A holoenzyme (*53*). PP2B could act in heart by reversing this or other analogously acting PP2A phosphorylations to decrease PP2A activity.

The A kinase anchor protein AKAP150 (corresponding to AKAP79 in humans and AKAP75 in cows) is the main AKAP at postsynaptic sites in brain (*54*, *55*). Ca_v1.2 is clustered at these sites (*56*, *57*), and AKAP150 coimmunoprecipitates with Ca_v1.2 from brain and heart (*8*, *58*, *59*). AKAP150 recruits PKA and PP2B to Ca_v1.2 in neurons (*52*, *58*, *60*, *61*). It also links PP2B and the adenylyl cyclases 5 and 6, but not PKA, to Ca_v1.2 in heart (*59*), where AKAP15/18 links PKA to Ca_v1.2 (*16*, *62*). Because AKAP150 binds not only to the C-terminus of $\alpha_1$1.2 but also to its N-terminus and its intracellular loop between domains I and II (*58*), AKAP150 and with it PP2B can bind simultaneously with AKAP15/18 to Ca_v1.2. In fact, AKAP150 is strictly required for coimmunoprecipitation of PP2B with Ca_v1.2 (*59*). The observation that peptide 5 does not displace PP2B from native Ca_v1.2 complexes could thus be due to the apparently stronger interaction of PP2B with Ca_v1.2 via AKAP150 than the direct PP2B binding to $\alpha_1$1.2. Accordingly, AKAP150 is necessary

for stable PP2B association with $Ca_v1.2$ although it is not clear whether it is sufficient. The lack of effect of peptide 5 on PP2B coimmunoprecipitation with $Ca_v1.2$ indicates at the first glance that the corresponding interaction is not required and the AKAP150-mediated interaction is sufficient but the lack of peptide 5 effect could be explained by a lack of access to this interaction site in the native complex.

Peptide 5 not only augments $I_{Ca}(L)$ under basal conditions but also enhances in absolute magnitude the increase in $I_{Ca}(L)$ by β-adrenergic stimulation with ISO. Accordingly, peptide 5 could act at least in part by enhancing the PKA-mediated increase in $Ca_v1.2$ activity. Our results also indicate that PP2A effectively reverses the PKA-stimulated activity of cardiac $Ca_v1.2$ only if bound to residues 1965−1970 and surrounding residues in $\alpha_1$1.2. An indirect implication of our results is that the phosphatase activity at $Ca_v1.2$ may be relatively high, keeping basal $I_{Ca}(L)$ activation low, limiting the extent of PKA-dependent current enhancement and potentially accelerating the reversal of current activation at the end of a bout of sympathetic activation.

In conclusion, there are at least two different attachment sites in the $Ca_v1.2$ channel complex for PP2A as defined by our CT-B and CT-8 constructs. The latter site is clearly important for negative regulation of $Ca_v1.2$ by PP2A, but the former site awaits yet more precise definition and functional studies.

ACKNOWLEDGMENT

The authors thank Dr. S. S. Taylor (HHMI, University of California San Diego) for providing the solid-phase peptide library and Dr. G. Walter (University of California San Diego) for an aliquot of the 6F9 antibody against PP2A/A.

SUPPORTING INFORMATION AVAILABLE

One figure showing that peptides 6−10, which are 10 residues long and cover peptides 4 and 5, do not inhibit PP2A and PP2B binding to GST-CT-8. This material is available free of charge via the Internet at http://pubs.acs.org.

REFERENCES

1. Marrion, N. V., and Tavalin, S. T. (1998) Selective activation of Ca^{2+}-activated K^+ channels by co-localized Ca^{2+}channels in hippocampal neurons. *Nature 395*, 900–905.
2. Grover, L. M., and Teyler, T. J. (1990) Two components of long-term potentiation induced by different patterns of afferent activation. *Nature 347*, 477–479.
3. Bolshakov, V. Y., and Siegelbaum, S. A. (1994) Postsynaptic induction and presynaptic expression of hippocampal long-term depression. *Science 264*, 148–152.
4. Christie, B. R., Schexnayder, L. K., and Johnston, D. (1997) Contribution of voltage-gated Ca^{2+} channels to homosynaptic long-term depression in the CA1 region in vitro. *J. Neurophysiol. 77*, 1651–1655.
5. Wang, H. X., Gerkin, R. C., Nauen, D. W., and Bi, G. Q. (2005) Coactivation and timing-dependent integration of synaptic potentiation and depression. *Nat. Neurosci. 8*, 187–193.
6. Ghosh, A., and Greenberg, M. E. (1995) Calcium signaling in neurons: molecular mechanisms and cellular consequences. *Science 268*, 239–247.
7. Dolmetsch, R. E., Pajvani, U., Fife, K., Spotts, J. M., and Greenberg, M. E. (2001) Signaling to the nucleus by an L-type calcium channel-calmodulin complex through the MAP kinase pathway. *Science 294*, 333–339.
8. Dai, S., Hall, D. D., and Hell, J. W. (2009) Supramolecular assemblies and localized regulation of voltage-gated ion channels. *Physiol. Rev. 89*, 411–452.
9. Reuter, H. (1983) Calcium channel modulation by neurotransmitters, enzymes and drugs. *Nature 301*, 569–574.
10. Bean, B. P., Nowycky, M. C., and Tsien, R. W. (1984) β-Adrenergic modulation of calcium channels in frog ventricular heart cells. *Nature 307*, 371–375.
11. Ono, K., and Fozzard, H. A. (1992) Phosphorylation restores activity of L-type calcium channels after rundown in inside-out patches from rabbit cardiac cells. *J. Physiol. 454*, 673–688.
12. Sculptoreanu, A., Rotman, E., Takahashi, M., Scheuer, T., and Catterall, W. A. (1993) Voltage-dependent potentiation of the activity of cardiac L-type calcium channel alpha 1 subunits due to phosphorylation by cAMP-dependent protein kinase. *Proc. Natl. Acad. Sci. U. S.A. 90*, 10135–10139.
13. Hall, D. D., Feekes, J. A., Arachchige Don, A. S., Shi, M., Hamid, J., Chen, L., Strack, S., Zamponi, G. W., Horne, M. C., and Hell, J. W. (2006) Binding of protein phosphatase 2A to the L-type calcium channel Cav1.2 next to Ser1928, its main PKA site, is critical for Ser1928 dephosphorylation. *Biochemistry 45*, 3448–3459.
14. Tandan, S., Wang, Y., Wang, T. T., Jiang, N., Hall, D. D., Hell, J. W., Luo, X., Rothermel, B. A., and Hill, J. A. (2009) Physical and functional interaction between calcineurin and the cardiac L-type Ca^{2+} channel. *Circ. Res. 105*, 51–60.
15. Hell, J. W. (2010) {beta}-Adrenergic regulation of the L-type Ca^{2+} channel CaV1.2 by PKA rekindles excitement. *Sci. Signal. 3*, pe33.
16. Fuller, M. D., Emrick, M. A., Sadilek, M., Scheuer, T., and Catterall, W. A. (2010) Molecular mechanism of calcium channel regulation in the fight-or-flight response. *Sci. Signal. 3*, ra70.
17. Ganesan, A. N., Maack, C., Johns, D. C., Sidor, A., and O'Rourke, B. (2006) Beta-adrenergic stimulation of L-type Ca^{2+} channels in cardiac myocytes requires the distal carboxyl terminus of alpha1C but not serine 1928. *Circ. Res. 98*, e11–18.
18. Lemke, T., Welling, A., Christel, C. J., Blaich, A., Bernhard, D., Lenhardt, P., Hofmann, F., and Moosmang, S. (2008) Unchanged beta-adrenergic stimulation of cardiac L-type calcium channels in Ca v 1.2 phosphorylation site S1928A mutant mice. *J. Biol. Chem. 283*, 34738–34744.
19. Yang, C. S., Vitto, M. J., Busby, S. A., Garcia, B. A., Kesler, C. T., Gioeli, D., Shabanowitz, J., Hunt, D. F., Rundell, K., Brautigan, D. L., and Paschal, B. M. (2005) Simian virus 40 small t antigen mediates conformation-dependent transfer of protein phosphatase 2A onto the androgen receptor. *Mol. Cell. Biol. 25*, 1298–1308.
20. Kremmer, E., Ohst, K., Kiefer, J., Brewis, N., and Walter, G. (1997) Separation of PP2A core enzyme and holoenzyme with monoclonal antibodies against the regulatory A subunit: abundant expression of both forms in cells. *Mol. Cell. Biol. 17*, 1692–1701.
21. Liang, H., Venema, V. J., Wang, X., Ju, H., Venema, R. C., and Marrero, M. B. (1999) Regulation of angiotensin II-induced phosphorylation of STAT3 in vascular smooth muscle cells. *J. Biol. Chem. 274*, 19846–19851.
22. Jicha, G. A., Weaver, C., Lane, E., Vianna, C., Kress, Y., Rockwood, J., and Davies, P. (1999) cAMP-dependent protein kinase phosphorylations on tau in Alzheimer's disease. *J. Neurosci. 19*, 7486–7494.
23. Davare, M. A., Dong, F., Rubin, C. S., and Hell, J. W. (1999) The A-kinase anchor protein MAP2B and cAMP-dependent protein kinase are associated with class C L-type calcium channels in neurons. *J. Biol. Chem. 274*, 30280–30287.
24. Burns-Hamuro, L. L., Ma, Y., Kammerer, S., Reineke, U., Self, C., Cook, C., Olson, G. L., Cantor, C. R., Braun, A., and Taylor, S. S. (2003) Designing isoform-specific peptide disruptors of protein kinase A localization. *Proc. Natl. Acad. Sci. U.S.A. 100*, 4072–4077.
25. Snutch, T. P., Tomlinson, W. J., Leonard, J. P., and Gilbert, M. M. (1991) Distinct calcium channels are generated by alternative splicing and are differentially expressed in the mammalian CNS. *Neuron 7*, 45–57.
26. Bennin, D. A., Don, A. S., Brake, T., McKenzie, J. L., Rosenbaum, H., Ortiz, L., DePaoli-Roach, A. A., and Horne, M. C. (2002) Cyclin G2 associates with protein phosphatase 2A catalytic and regulatory B′ subunits in active complexes and induces nuclear aberrations and a G1/S phase cell cycle arrest. *J. Biol. Chem. 277*, 27449–27467.
27. Mondragon, A., Griffith, E. C., Sun, L., Xiong, F., Armstrong, C., and Liu, J. O. (1997) Overexpression and purification of human calcineurin alpha from *Escherichia coli* and assessment of catalytic functions of residues surrounding the binuclear metal center. *Biochemistry 36*, 4934–4942.
28. Davare, M. A., and Hell, J. W. (2003) Increased phosphorylation of the neuronal L-type Ca(2+) channel Ca(v)1.2 during aging. *Proc. Natl. Acad. Sci. U.S.A. 100*, 16018–16023.
29. Geladopoulos, T. P., Sotiroudis, T. G., and Evangelopoulos, A. E. (1991) A malachite green colorimetric assay for protein phosphatase activity. *Anal. Biochem. 192*, 112–116.
30. Harder, K. W., Owen, P., Wong, L. K., Aebersold, R., Clark-Lewis, I., and Jirik, F. R. (1994) Characterization and kinetic analysis of the intracellular domain of human protein tyrosine phosphatase beta (HPTP beta) using synthetic phosphopeptides. *Biochem. J. 298*, 395–401.

31. Fathi, A. R., Krautheim, A., Lucke, S., Becker, K., and Juergen Steinfelder, H. (2002) Nonradioactive technique to measure protein phosphatase 2A-like activity and its inhibition by drugs in cell extracts. *Anal. Biochem. 310*, 208–214.
32. Wiechen, K., Yue, D. T., and Herzig, S. (1995) Two distinct functional effects of protein phosphatase inhibitors on guinea-pig cardiac L-type Ca^{2+} channels. *J. Physiol.* (*London*) *484*, 583–592.
33. Sun, J., Picht, E., Ginsburg, K. S., Bers, D. M., Steenbergen, C., and Murphy, E. (2006) Hypercontractile female hearts exhibit increased S-nitrosylation of the L-type Ca^{2+} channel alpha1 subunit and reduced ischemia/reperfusion injury. *Circ. Res. 98*, 403–411.
34. Fan, J. S., and Palade, P. (1998) Perforated patch recording with beta-escin. *Pfluegers Arch. 436*, 1021–1023.
35. Shi, Y. (2009) Serine/threonine phosphatases: mechanism through structure. *Cell 139*, 468–484.
36. Davare, M. A., Horne, M. C., and Hell, J. W. (2000) Protein phosphatase 2A is associated with class C L-type calcium channels ($Ca_v1.2$) and antagonizes channel phosphorylation by cAMP-dependent protein kinase. *J. Biol. Chem. 275*, 39710–39717.
37. McCright, B., Rivers, A. M., Audlin, S., and Virshup, D. M. (1996) The B56 family of protein phosphatase 2A (PP2A) regulatory subunits encodes differentiation-induced phosphoproteins that target PP2A to both nucleus and cytoplasm. *J. Biol. Chem. 271*, 22081–22089.
38. Price, N. E., and Mumby, M. C. (1999) Brain protein serine/threonine phosphatases. *Curr. Opin. Neurobiol. 9*, 336–342.
39. Marx, S. O., Reiken, S., Hisamatsu, Y., Gaburjakova, M., Gaburjakova, J., Yang, Y. M., Rosemblit, N., and Marks, A. R. (2001) Phosphorylation-dependent regulation of ryanodine receptors: a novel role for leucine/isoleucine zippers. *J. Cell Biol. 153*, 699–708.
40. Hess, P., Lansman, J. B., and Tsien, R. W. (1984) Different modes of Ca channel gating behaviour favoured by dihydropyridine Ca agonists and antagonists. *Nature 311*, 538–544.
41. Trautwein, W., and Hescheler, J. (1990) Regulation of cardiac L-type calcium current by phosphorylation and G proteins. *Annu. Rev. Physiol. 52*, 257–274.
42. Ono, K., and Fozzard, H. A. (1993) Two phosphatase sites on the Ca^{2+} channel affecting different kinetic functions. *J Physiol 470*, 73–84.
43. Groschner, K., Schuhmann, K., Mieskes, G., Baumgartner, W., and Romanin, C. (1996) A type 2A phosphatase-sensitive phosphorylation site controls modal gating of L-type Ca^{2+} channels in human vascular smooth-muscle cells. *Biochem. J. 318*, 513–517.
44. duBell, W. H., Wright, P. A., Lederer, W. J., and Rogers, T. B. (1997) Effect of the immunosupressant FK506 on excitation-contraction coupling and outward K^+ currents in rat ventricular myocytes. *J. Physiol. 501*, 509–516.
45. McCall, E., Li, L., Satoh, H., Shannon, T. R., Blatter, L. A., and Bers, D. M. (1996) Effects of FK-506 on contraction and Ca^{2+} transients in rat cardiac myocytes. *Circ. Res. 79*, 1110–1121.
46. Yatani, A., Honda, R., Tymitz, K. M., Lalli, M. J., and Molkentin, J. D. (2001) Enhanced Ca^{2+} channel currents in cardiac hypertrophy induced by activation of calcineurin-dependent pathway. *J. Mol. Cell. Cardiol. 33*, 249–259.
47. Su, Z., Sugishita, K., Li, F., Ritter, M., and Barry, W. H. (2003) Effects of FK506 on $[Ca^{2+}]i$ differ in mouse and rabbit ventricular myocytes. *J. Pharmacol. Exp. Ther. 304*, 334–341.
48. Fauconnier, J., Lacampagne, A., Rauzier, J. M., Fontanaud, P., Frapier, J. M., Sejersted, O. M., Vassort, G., and Richard, S. (2005) Frequency-dependent and proarrhythmogenic effects of FK-506 in rat ventricular cells. *Am. J. Physiol. Heart Circ. Physiol. 288*, H778–786.
49. Santana, L. F., Chase, E. G., Votaw, V. S., Nelson, M. T., and Greven, R. (2002) Functional coupling of calcineurin and protein kinase A in mouse ventricular myocytes. *J. Physiol. 544*, 57–69.
50. Burley, J. R., and Sihra, T. S. (2000) A modulatory role for protein phosphatase 2B (calcineurin) in the regulation of Ca^{2+} entry. *Eur. J. Neurosci. 12*, 2881–2891.
51. Lukyanetz, E. A., Piper, T. P., and Sihra, T. S. (1998) Calcineurin involvement in the regulation of high-threshold Ca^{2+} channels in NG108-15 (rodent neuroblastoma x glioma hybrid) cells. *J. Physiol. 510*, 371–385.
52. Oliveria, S. F., Dell'acqua, M. L., and Sather, W. A. (2007) AKAP79/150 anchoring of calcineurin controls neuronal L-type Ca(2+) channel activity and nuclear signaling. *Neuron 55*, 261–275.
53. Ahn, J. H., McAvoy, T., Rakhilin, S. V., Nishi, A., Greengard, P., and Nairn, A. C. (2007) Protein kinase A activates protein phosphatase 2A by phosphorylation of the B56delta subunit. *Proc. Natl. Acad. Sci. U.S.A. 104*, 2979–2984.
54. Lu, Y., Allen, M., Halt, A. R., Weisenhaus, M., Dallapiazza, R. F., Hall, D. D., Usachev, Y. M., McKnight, G. S., and Hell, J. W. (2007) Age-dependent requirement of AKAP150-anchored PKA and GluR2-lacking AMPA receptors in LTP. *EMBO J. 26*, 4879–4890.
55. Weisenhaus, M., Allen, M. L., Yang, L., Lu, Y., Nichols, C. B., Su, T., Hell, J. W., and McKnight, G. S. (2010) Mutations in AKAP5 disrupt dendritic signaling complexes and lead to electrophysiological and behavioral phenotypes in mice. *PLoS One 5*, e10325.
56. Davare, M. A., Avdonin, V., Hall, D. D., Peden, E. M., Burette, A., Weinberg, R. J., Horne, M. C., Hoshi, T., and Hell, J. W. (2001) A beta2 adrenergic receptor signaling complex assembled with the Ca^{2+} channel Cav1.2. *Science 293*, 98–101.
57. Obermair, G. J., Szabo, Z., Bourinet, E., and Flucher, B. E. (2004) Differential targeting of the L-type Ca^{2+} channel alpha1C (CaV1.2) to synaptic and extrasynaptic compartments in hippocampal neurons. *Eur. J. Neurosci. 19*, 2109–2122.
58. Hall, D. D., Davare, M. A., Shi, M., Allen, M. L., Weisenhaus, M., McKnight, G. S., and Hell, J. W. (2007) Critical role of cAMP-dependent protein kinase anchoring to the L-type calcium channel Cav1.2 via A-kinase anchor protein 150 in neurons. *Biochemistry 46*, 1635–1646.
59. Nichols, C. B., Rossow, C. F., Navedo, M. F., Westenbroek, R. E., Catterall, W. A., Santana, L. F., and McKnight, G. S. (2010) Sympathetic stimulation of adult cardiomyocytes requires association of AKAP5 with a subpopulation of L-type calcium channels. *Circ. Res. 107*, 747–756.
60. Coghlan, V. M., Perrino, B. A., Howard, M., Langeberg, L. K., Hicks, J. B., Gallatin, W. M., and Scott, J. D. (1995) Association of protein kinase A and protein phosphatase 2B with a common anchoring protein. *Science,* 108–111.
61. Oliveria, S. F., Gomez, L. L., and Dell'Acqua, M. L. (2003) Imaging kinase−AKAP79−phosphatase scaffold complexes at the plasma membrane in living cells using FRET microscopy. *J. Cell Biol. 160*, 101–112.
62. Hulme, J. T., Lin, T. W., Westenbroek, R. E., Scheuer, T., and Catterall, W. A. (2003) Beta-adrenergic regulation requires direct anchoring of PKA to cardiac CaV1.2 channels via a leucine zipper interaction with a kinase-anchoring protein 15. *Proc. Natl. Acad. Sci. U.S.A. 100*, 13093–13098.